A Mean-Field Model for TRIP - Algorithms and Parameter Identification

M. Petersmann [1], G. Cailletaud [2], T. Antretter [1], U. Ehlenbröcker [3]

[1]Montanuniversitaet Leoben, Institute of Mechanics, Franz-Josef Straße 18 8700 Leoben, Austria
[2]MINES ParisTech, MAT-Centre des Matériaux, CNRS UMR 7633, BP 87 91003 Evry, France
[3]University of Paderborn, Chair of Mechanics, Warburger Straße 100, 33100 Paderborn, Germany

Introduction and Motivation

Experimentally observed, **backflow** [1] motivated the introduction of a **backstress** in constitutive models, to depict non-proportional loading paths [2]. This backstress is related to the selection of interacting **crystallographic variants**, changing as a function of the applied load direction and the **interaction between variants and dislocations**.

We present coupling strategies for the phase transformation and plasticity at different scales. A **meso-macro** model for structural calculations has been set up, which however needs to become more flexible. Therefore, a **micro-meso** model is developed, where individual martensite shape strains from crystallographic calculations (see [3]) are resolved.

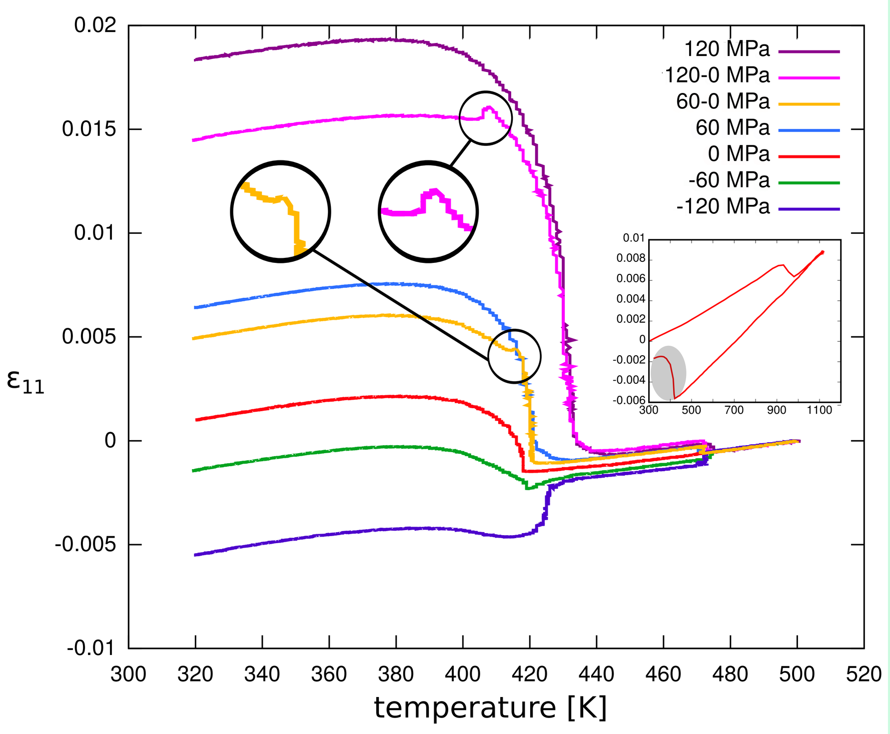

Open dilatometric loop without loading. Experimentally observed backflow upon unloading.

Results

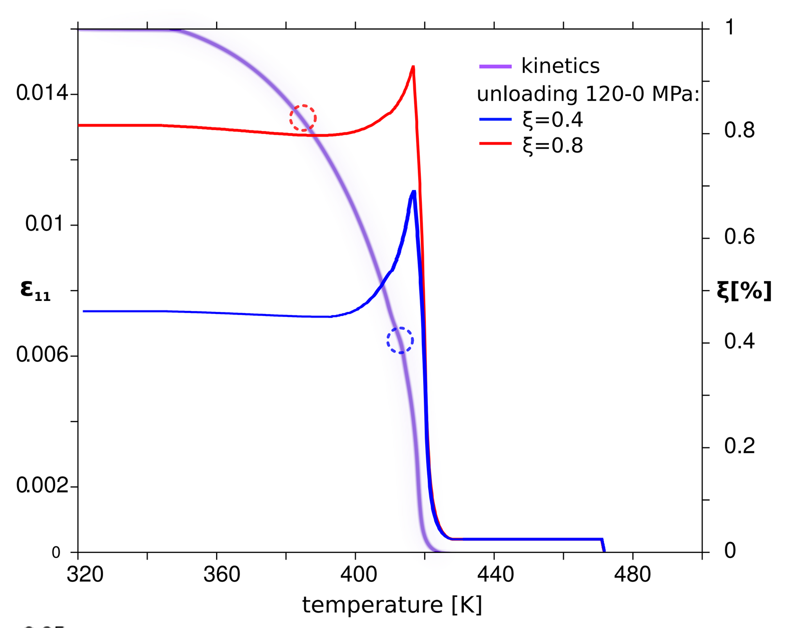

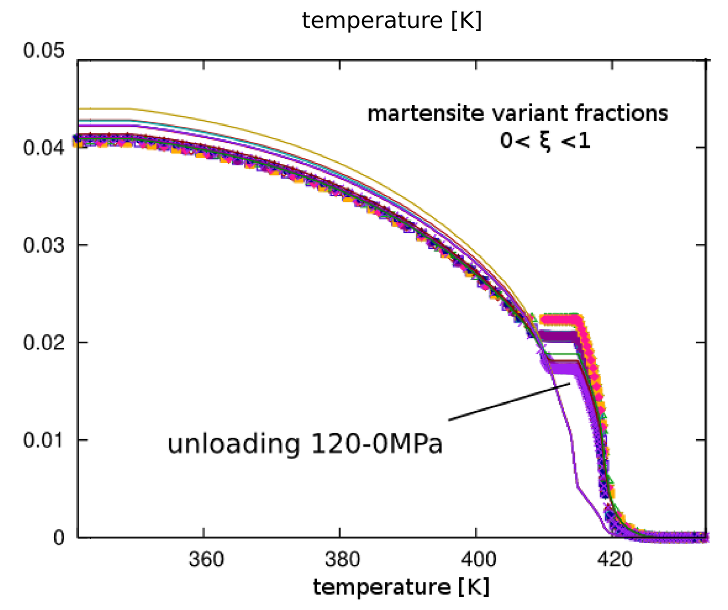

- While experimentally it is difficult to unload at low martensite phase fraction (due to the high necessary cooling rates to form martensite), simulations confirm that the backflow upon unloading at these is significantly higher.
- In the micro-meso model the information on the variant fractions is directly available and can be adapted to fit variant statistics optained from EBSD.

Conclusions

- An ample meso-macro model has been implicitly implemented for the use in structural FEM calculations.
- A physically based micro-meso model has been set up as an additional layer in the multi-scale modeling chain. It provides additional information that is not experimentally accessible (e.g. relative amounts of plastic- and transformation strain). This opens new possibilities to formulate and calibrate hardening laws and improve parameter identification for macro models.

References

[1] K Nagayama, T Terasaki, K Tanaka, FD Fischer, T Antretter, G Cailletaud, and F Azzouz. Mechanical properties of a cr–ni–mo–al–ti maraging steel in the process of martensitic transformation. *Materials Science and Engineering: A*, 308(1):25–37, 2001.

[2] M. Fischlschweiger, C. Cailletaud, and Antretter T. A mean-field model for transformation induced plasticity including backstress effects for non-proportional loadings. *International journal of plasticity*, pages 53–71, 2012.

[3] Liang Qi, A.G. Khachaturyan, and J.W. Morris Jr. The microstructure of dislocated martensitic steel: Theory. *Acta Materialia*, 76(0):23 – 39, 2014.

[4] G. Cailletaud. *Une approche microméchanique phénoménologique du comportement inélastique des métaux*. PhD thesis, Université Paris 6., 1987.

[5] Christian Lexcellent and Anja Schlömerkemper. Comparison of several models for the determination of the phase transformation yield surface in shape-memory alloys with experimental data. *Acta materialia*, 55(9):2995–3006, 2007.

Acknowledgements

Financial support by the Austrian Federal Government (in particular from Bundesministerium für Verkehr, Innovation und Technologie and Bundesministerium für Wissenschaft, Forschung und Wirtschaft) represented by Österreichische Forschungsförderungsgesellschaft mbH and the Styrian and the Tyrolean Provincial Government, represented by Steirische Wirtschaftsförderungsgesellschaft mbH and Standortagentur Tirol, within the framework of the COMET Funding Programme is gratefully acknowledged.

Competence Centers for Excellent Technologies

Meso-macro model features and algorithms

Structure of **Jacobian** [**J**] in meso-macro model [2] for Newton-Raphson scheme.

R...Residual, A...Austenite, M...Martensite, O...orientational part of transformation strain

$$[\mathbf{J}] = \begin{array}{|c|c|c|c|c|c|c|c|c|c|c|}
\hline
\frac{\partial \mathbf{R}^{\varepsilon}}{\partial\Delta\bar{\underset{\sim}{\varepsilon}}^e} & \frac{\partial \mathbf{R}^{\varepsilon}}{\partial\Delta p^a} & \frac{\partial \mathbf{R}^{\varepsilon}}{\partial\Delta p^m} & \frac{\partial \mathbf{R}^{\varepsilon}}{\partial\Delta p^o} & \frac{\partial \mathbf{R}^{\varepsilon}}{\partial\Delta\bar{\underset{\sim}{\varepsilon}}^o} & \underset{\sim}{\mathbf{0}} & \underset{\sim}{\mathbf{0}} & \frac{\partial \mathbf{R}^{\varepsilon}}{\partial\Delta\underset{\sim}{\alpha}^a} & \frac{\partial \mathbf{R}^{\varepsilon}}{\partial\Delta\underset{\sim}{\alpha}^m} & \frac{\partial \mathbf{R}^{\varepsilon}}{\partial\Delta\underset{\sim}{\alpha}^o} & \frac{\partial \mathbf{R}^{\varepsilon}}{\partial\Delta\xi} \\
\hline
\frac{\partial \mathbf{R}^{p^a}}{\partial\Delta\bar{\underset{\sim}{\varepsilon}}^e} & \frac{\partial \mathbf{R}^{p^a}}{\partial\Delta p^a} & 0 & 0 & \underset{\sim}{\mathbf{0}} & \underset{\sim}{\mathbf{0}} & \underset{\sim}{\mathbf{0}} & \frac{\partial \mathbf{R}^{p^a}}{\partial\Delta\underset{\sim}{\alpha}^a} & \underset{\sim}{\mathbf{0}} & \frac{\partial \mathbf{R}^{p^a}}{\partial\Delta\underset{\sim}{\alpha}^o} & 0 \\
\hline
\frac{\partial \mathbf{R}^{p^m}}{\partial\Delta\bar{\underset{\sim}{\varepsilon}}^e} & 0 & \frac{\partial \mathbf{R}^{p^m}}{\partial\Delta p^m} & 0 & \underset{\sim}{\mathbf{0}} & \underset{\sim}{\mathbf{0}} & \underset{\sim}{\mathbf{0}} & \underset{\sim}{\mathbf{0}} & \frac{\partial \mathbf{R}^{p^m}}{\partial\Delta\underset{\sim}{\alpha}^m} & \underset{\sim}{\mathbf{0}} & 0 \\
\hline
\frac{\partial \mathbf{R}^{p^o}}{\partial\Delta\bar{\underset{\sim}{\varepsilon}}^e} & 0 & 0 & \frac{\partial \mathbf{R}^{p^o}}{\partial\Delta p^o} & \underset{\sim}{\mathbf{0}} & \underset{\sim}{\mathbf{0}} & \underset{\sim}{\mathbf{0}} & \frac{\partial \mathbf{R}^{p^o}}{\partial\Delta\underset{\sim}{\alpha}^a} & \underset{\sim}{\mathbf{0}} & \frac{\partial \mathbf{R}^{p^o}}{\partial\Delta\underset{\sim}{\alpha}^o} & \frac{\partial \mathbf{R}^{p^o}}{\partial\Delta\xi} \\
\hline
\frac{\partial \mathbf{R}^{\varepsilon^o}}{\partial\Delta\bar{\underset{\sim}{\varepsilon}}^e} & \underset{\sim}{\mathbf{0}} & \underset{\sim}{\mathbf{0}} & \frac{\partial \mathbf{R}^{\varepsilon^o}}{\partial\Delta p^o} & -\underset{\approx}{\mathbf{I}} & \underset{\sim}{\mathbf{0}} & \underset{\sim}{\mathbf{0}} & \frac{\partial \mathbf{R}^{\varepsilon^o}}{\partial\Delta\underset{\sim}{\alpha}^a} & \underset{\sim}{\mathbf{0}} & \frac{\partial \mathbf{R}^{\varepsilon^o}}{\partial\Delta\underset{\sim}{\alpha}^o} & \frac{\partial \mathbf{R}^{\varepsilon^o}}{\partial\Delta\xi} \\
\hline
\frac{\partial \mathbf{R}^{\beta^a}}{\partial\Delta\bar{\underset{\sim}{\varepsilon}}^e} & \frac{\partial \mathbf{R}^{\beta^a}}{\partial\Delta p^a} & \underset{\sim}{\mathbf{0}} & \underset{\sim}{\mathbf{0}} & \underset{\approx}{\mathbf{0}} & \frac{\partial \mathbf{R}^{\beta^a}}{\partial\Delta\underset{\sim}{\beta}^a} & \underset{\approx}{\mathbf{0}} & \frac{\partial \mathbf{R}^{\beta^a}}{\partial\Delta\underset{\sim}{\alpha}^a} & \underset{\approx}{\mathbf{0}} & \frac{\partial \mathbf{R}^{\beta^a}}{\partial\Delta\underset{\sim}{\alpha}^o} & \underset{\sim}{\mathbf{0}} \\
\hline
\frac{\partial \mathbf{R}^{\beta^{mo}}}{\partial\Delta\bar{\underset{\sim}{\varepsilon}}^e} & \underset{\sim}{\mathbf{0}} & \frac{\partial \mathbf{R}^{\beta^{mo}}}{\partial\Delta p^m} & \frac{\partial \mathbf{R}^{\beta^{mo}}}{\partial\Delta p^o} & \underset{\approx}{\mathbf{0}} & \underset{\approx}{\mathbf{0}} & \frac{\partial \mathbf{R}^{\beta^{mo}}}{\partial\Delta\underset{\sim}{\beta}^{mo}} & \frac{\partial \mathbf{R}^{\beta^{mo}}}{\partial\Delta\underset{\sim}{\alpha}^a} & \frac{\partial \mathbf{R}^{\beta^{mo}}}{\partial\Delta\underset{\sim}{\alpha}^m} & \frac{\partial \mathbf{R}^{\beta^{mo}}}{\partial\Delta\underset{\sim}{\alpha}^o} & \frac{\partial \mathbf{R}^{\beta^{mo}}}{\partial\Delta\xi} \\
\hline
\frac{\partial \mathbf{R}^{\alpha^a}}{\partial\Delta\bar{\underset{\sim}{\varepsilon}}^e} & \frac{\partial \mathbf{R}^{\alpha^o}}{\partial\Delta p^a} & \underset{\sim}{\mathbf{0}} & \underset{\sim}{\mathbf{0}} & \underset{\approx}{\mathbf{0}} & \underset{\approx}{\mathbf{0}} & \underset{\approx}{\mathbf{0}} & \frac{\partial \mathbf{R}^{\alpha^a}}{\partial\Delta\underset{\sim}{\alpha}^a} & \underset{\approx}{\mathbf{0}} & \frac{\partial \mathbf{R}^{\alpha^a}}{\partial\Delta\underset{\sim}{\alpha}^o} & \underset{\sim}{\mathbf{0}} \\
\hline
\frac{\partial \mathbf{R}^{\alpha^m}}{\partial\Delta\bar{\underset{\sim}{\varepsilon}}^e} & \underset{\sim}{\mathbf{0}} & \frac{\partial \mathbf{R}^{\alpha^m}}{\partial\Delta p^m} & \underset{\sim}{\mathbf{0}} & \underset{\approx}{\mathbf{0}} & \underset{\approx}{\mathbf{0}} & \underset{\approx}{\mathbf{0}} & \underset{\approx}{\mathbf{0}} & \frac{\partial \mathbf{R}^{\alpha^m}}{\partial\Delta\underset{\sim}{\alpha}^m} & \underset{\approx}{\mathbf{0}} & \underset{\sim}{\mathbf{0}} \\
\hline
\frac{\partial \mathbf{R}^{\alpha^o}}{\partial\Delta\bar{\underset{\sim}{\varepsilon}}^e} & \underset{\sim}{\mathbf{0}} & \underset{\sim}{\mathbf{0}} & \frac{\partial \mathbf{R}^{\alpha^o}}{\partial\Delta p^o} & \underset{\approx}{\mathbf{0}} & \underset{\approx}{\mathbf{0}} & \underset{\approx}{\mathbf{0}} & \frac{\partial \mathbf{R}^{\alpha^o}}{\partial\Delta\underset{\sim}{\alpha}^a} & \underset{\approx}{\mathbf{0}} & \frac{\partial \mathbf{R}^{\alpha^o}}{\partial\Delta\underset{\sim}{\alpha}^o} & \frac{\partial \mathbf{R}^{\alpha^o}}{\partial\Delta\xi} \\
\hline
\frac{\partial \mathbf{R}^{\xi}}{\partial\Delta\bar{\underset{\sim}{\varepsilon}}^e} & \frac{\partial \mathbf{R}^{\xi}}{\partial\Delta p^a} & 0 & 0 & \frac{\partial \mathbf{R}^{\xi}}{\partial\Delta\bar{\underset{\sim}{\varepsilon}}^o} & \underset{\approx}{\mathbf{0}} & \underset{\approx}{\mathbf{0}} & \frac{\partial \mathbf{R}^{\xi}}{\partial\Delta\underset{\sim}{\alpha}^a} & \underset{\approx}{\mathbf{0}} & \frac{\partial \mathbf{R}^{\xi}}{\partial\Delta\underset{\sim}{\alpha}^o} & \frac{\partial \mathbf{R}^{\xi}}{\partial\Delta\xi} \\
\hline
\end{array}$$

$\Delta\bar{\underset{\sim}{\xi}}(\Delta\bar{\underset{\sim}{\varepsilon}}^e, \xi, \bar{\underset{\sim}{\varepsilon}}^{p^{A,M}}, \Delta\xi; \bar{\underset{\sim}{\varepsilon}}^{vol}, \bar{\underset{\sim}{\varepsilon}}^o)$

$p^{A,M}$ viscoplastic formulation

Orientation strain (transform.)

Stress scaling rules $\underset{\sim}{\beta}^{A,M}$ [4]

Interacting backstresses $\underset{\sim}{\alpha}^{A,M,O}$

Transformation kinetics

- Strain-driven process in finite element program - computation of state variables at t^{n+1} by means of the internal variables at time t^n and the current strain tensor.
- Return mapping/projection scheme to solve linearized system of equations.
- Coupling between plastic deformation and orientation mechanism via a backstress.
- Hardening law based on phase fraction must reproduce experimentally accessible kinetics. Proposition: Inverse of fitted kinetics function with *tanh* or combination of *ln*'s.

Numerical Parameter Identification

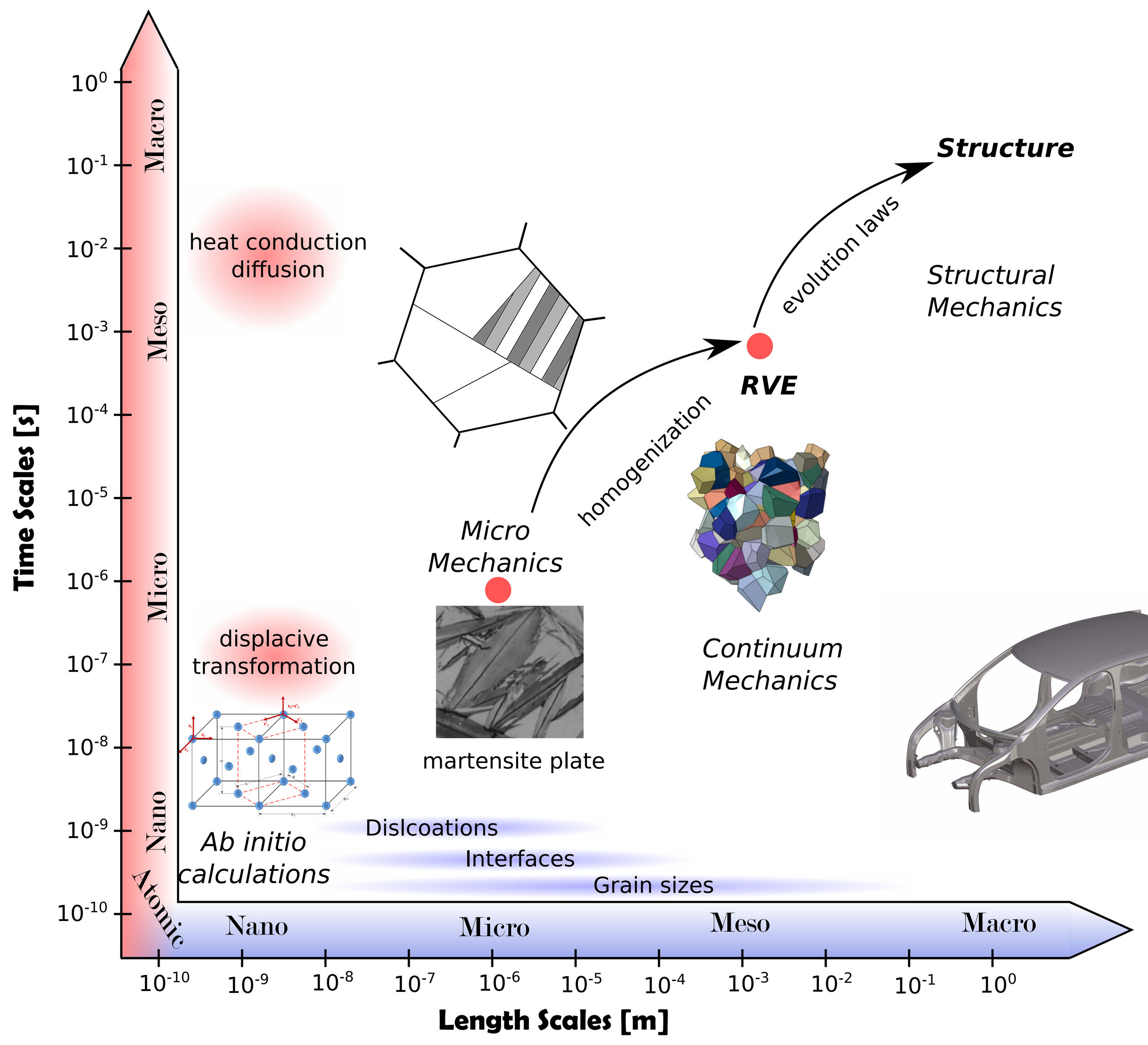

Overview of the length- and time scales to capture the TRIP phenomenon. The red points mark the scales where the micro-meso or meso-macro models are formulated respectively. An upscaling to the rescpective higher scale is done via a stress scaling or scale-transition rule (β-rule [4]).

Micro-meso Model:

Crystal plasticity:

$$\Delta\underset{\sim}{\varepsilon}^p = \xi^i \sum_s \Delta p^s \eta^s \underset{\sim}{\mathbf{m}}^s$$

Variant selection:

$$\Delta\underset{\sim}{\varepsilon}^t = \underset{\sim}{\sigma}^a : \underset{\sim}{\varepsilon}^t_i + V^{int}$$

V^{int}:

-Variant interaction: $\xi^i \xi^j H^{ij}$

-Variant-Slip interaction $\xi^i(1 - \mathbf{h}^i \cdot \mathbf{n}^j)$

$\mathbf{n}^j$... slip-plane vector

The anisotropic macro yield-function based on the Lode-angle can be fitted to a theoretical yield function obtained from crystallographic transformation strains as in [5]. The strains are calculated in accordance with the hierarchical, microstructural arrangement into **Packets** (that are divided into **Blocks** of two **Variants** respectively) in low-carbon steels [3]. There are some good/similar solutions in the sense that they all fulfill the subsequent criteria:

$$\mathcal{P}^{\text{cubic}} \times \begin{pmatrix} 1.070 & 0.071 & -0.071 \\ 0.071 & 1.072 & -0.071 \\ 0.125 & 0.125 & 0.880 \end{pmatrix}$$

i) Deviation of habit-plane $\mathbf{h}^i$ from $\{111\}_\gamma \approx 0$ as experimentally supported by almost all examples of low-carbon steels. **ii)** Slip density is reasonably large. **iii)** Shape strain $\varepsilon_0 = \lambda_1(\mathbf{F}) - \lambda_3(\mathbf{F})$ is small. **iv)** Orientation relationship is between Kurdjumov-Sachs and Nishiyama-Wassermann.

The above given deformation matrix is an average over these solutions to be representative for the microstructure. Using these deformations, we propose a constitutive model incorporating crystal plasticity on the microscale and formulate an interaction matrix based on the hierarchical structure. The model should **i)** bridge the gap between RVE calculations of individual inclusions with **Block**-deformations (shown on the right) and the meso-macro model by quantitatively predicting the amounts of plastic- and transformation strain, as well as **ii)** generate more data to make the meso-macro model more flexible.

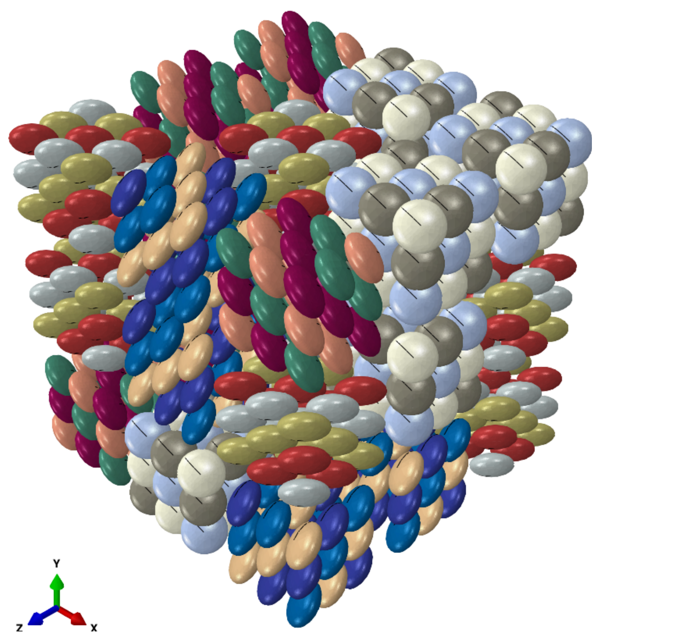

Hierarchical RVE of Blocks forming Packets typical for low carbon steel.